# On the Feasibility of All-solid-state Batteries with LLZO as a Single Electrolyte



**Author(s):**
Kravchyk, Kostiantyn V.; Karabay, Dogan Tarik; Kovalenko, Maksym V.

**Publication date:**
2021-10-29

**Permanent link:**
https://doi.org/10.3929/ethz-b-000524539



**Originally published in:**
Research Square, https://doi.org/10.21203/rs.3.rs-1020785/v1

# On the Feasibility of All-solid-state Batteries with LLZO as a Single Electrolyte

**Kostiantyn V. Kravchyk**
ETH Zürich
**Dogan Tarik Karabay**
ETH Zürich
**Maksym V. Kovalenko** ( mvkovalenko@ethz.ch )
ETH Zürich

**Research Article**

**Keywords:** Li-garnet solid-state battery, LLZO solid-state electrolyte, energy density, power density

**Posted Date:** October 29th, 2021

**DOI:** https://doi.org/10.21203/rs.3.rs-1020785/v1



**Version of Record:** A version of this preprint was published at Scientific Reports on January 21st, 2022.
See the published version at https://doi.org/10.1038/s41598-022-05141-x.

# Abstract

Replacement of Li-ion liquid-state electrolytes by solid-state counterparts in a Li-ion battery (LIB) is a major research objective as well as an urgent priority for the industry, as it enables the use of a Li metal anode and provides new opportunities to realize safe, non-flammable, and temperature-resilient batteries. Among the plethora of solid-state electrolytes (SSEs) investigated, garnet-type Li-ion electrolytes based on cubic $Li_7La_3Zr_2O_{12}$ (LLZO) are considered the most appealing candidates for the development of future solid-state batteries because of their low electronic conductivity of *ca*. $10^{-8}$ S $cm^{-1}$ (RT) and a wide electrochemical operation window of 0 – 6 V *vs.* $Li^+$/Li. However, high LLZO density (5.1 g $cm^{-3}$) and its lower level of Li-ion conductivity (up to 1 mS $cm^{-1}$ at RT) compared to liquid electrolytes (1.28 g $cm^{-3}$; ca. 10 mS $cm^{-1}$ at RT) still raise the question as to the feasibility of using solely LLZO as an electrolyte for achieving competitive energy and power densities. In this work, we analyzed the energy densities of Li-garnet all-solid-state batteries based solely on LLZO SSE by modeling their Ragone plots using $LiCoO_2$ as the model cathode material. This assessment allowed us to identify values of the LLZO thickness, cathode areal capacity, and LLZO content in the solid-state cathode required to match the energy density of conventional lithium-ion batteries (ca. 180 Wh $kg^{-1}$ and 497 Wh $L^{-1}$) at the power densities of 200 W $kg^{-1}$ and 600 W $L^{-1}$, corresponding to *ca*. 1h of battery discharge time (1C). We then discuss key challenges in the practical deployment of LLZO SSE in the fabrication of Li-garnet all-solid-state batteries.


# Introduction

In a search for non-flammable and non-toxic energy storage systems that possess high energy and power densities, all-solid-state batteries based on $Li_7La_3Zr_2O_{12}$ (LLZO) solid-state electrolyte (SSE) have come into a major research spotlight.[1–11] LLZO SSE has numerous advantages such as low electronic conductivity of *ca*. $10^{-8}$ S $cm^{-1}$ (RT),[12] high chemical and thermal stabilities. Moreover, contrary to other Li-ion conducting SSEs, LLZO has a wide electrochemical voltage window of 0 – 6 V *vs.* $Li^+$/Li (obtained in the experimental operation),[13] enabling its employment in combination with the metallic lithium anode and utilization of high-voltage cathodes.

While broad attention to Li-garnet solid-state batteries (SSBs) is surely helpful for the progress in this area,[14–18] analysis of the literature appoints to the lack of clear opinion in the research community as to the configuration of future Li-garnet SSBs. On the one hand, the researchers are mostly united with the idea that LLZO SSE should face Li metal anode, enabling to mitigate the formation of the Li dendrites (when necessary pressure is applied).[19–23] On the other hand, opinions on the design of the cathode layer are more divergent. Proposed are additions of LLZO[24–32] or other electrolytes (ionic liquids,[33–37] or polymers[38]). Considering the ongoing debates on compelling Li-garnet SSB configurations, we first analyze the very first battery structure containing LLZO as the only SSE, as schematically depicted in Figure 1. Specifically, we intend to shed light on whether this approach is feasible, given high LLZO density (5.1 g $cm^{-3}$) and a mediocre level of its Li-ion conductivity as compared to liquid electrolytes (up

to 1 mS $cm^{-1}$ at RT),[1,2,8,39] The resulting impact of both factors requires the employment of high LLZO content in the cathode for reaching high power density, which in turn leads to the need for much higher areal capacities of solid-state cathodes as compared to the conventional counterparts for achieving same energy densities.[40] These energy/power density tradeoff considerations point to severe limitations on the LLZO content used in the solid-state cathode and cast doubt on even the feasibility of a solely LLZO approach.

In this work, taking 18650 Panasonic (231 Wh $kg^{-1}$, 636Wh $L^{-1}$)[41] and Samsung (180 Wh $kg^{-1}$, 497 Wh $L^{-1}$)[42] batteries as reference systems for defining acceptable energy density/power density balance, we assess areal capacities of Li-garnet solid-state cathodes, LLZO cathode content and LLZO thicknesses required to match their energy densities at a power density of 200 W $kg^{-1}$ and 600 W $L^{-1}$ (corresponding to ca. 1h of discharge) through the simulation of Ragone plots. We discuss the critical interplay between all variables along with the calculation of their respective minimal and maximal values (break-even points). Among various possible cathode materials, the choice of cathode active material was limited to $LiCoO_2$, due to its high electronic and Li-ion conductivity in both lithiated and delithiated states.[43–46] We then review in detail other factors hindering the commercial deployment of Li-garnet SSBs, such as volume changes of Li upon its plaiting/stripping, and the difficulties associated with the fabrication of LLZO based solid-state cathodes, giving our perspective on these problems.

## Results And Discussion

# Energy and power densities of Li-garnet SSBs

To assess achievable energy and power density of Li-garnet SSBs, 1D-isothermal lithium-ion battery model with single-ion conducting solid electrolyte developed by COMSOL Multiphysics[47,48] was applied to simulate their electrochemical performance during discharge. All equations governing the simulation can be found in the Supporting Information. The schematic of the model is depicted in Figure S1. Parameters used for simulation are summarized in Table S2. The following compositions of LCO-LLZO solid-state cathodes were modeled: 70 vol.% of LCO - 30 vol.% of LLZO, 60 vol.% of LCO - 40 vol.% of LLZO, 50 vol.% of LCO - 50 vol.% of LLZO and 40 vol.% of LCO - 60 vol.% of LLZO. Of note, in these simulations, we considered that no interfacial resistance is present at both LLZO/Li and LLZO/LCO interfaces, and no porosity was assumed to exist in the solid-state cathodes. Clearly, these conditions are oversimplified, but they enable to assess the highest reachable limits of energy and the power density of Li/LLZO/LCO SSBs. The simulation data obtained for the exemplary systems considering LLZO/Li (0.1 Ω $cm^2$)[49] and LLZO/LCO (50 Ω $cm^2$)[50] interfacial resistances, as well as the porosity in LCO/LLZO solid-state cathode, can be found in the Supporting Information.

Simulations were performed varying (i) the areal capacity of the cathode layer (0.5-5 mAh $cm^{-2}$), (ii) the thickness of LLZO dense layer separating the cathode and Li anode layers (0.1- 90 µm), (iii) the temperature (30°C and 70°C), and (iv) the C-rate (0.5C-5C). Examples of the resulting voltage profiles

simulated at different C-rates, cathode areal capacity of 4 mAh $cm^{-2}$, and LLZO thicknesses of 30 μm are shown in Figures 2a and 2b (see Supporting Information, Figures S2-S25, for a complete set of simulated voltage profiles). The achievable energy and power densities were calculated from simulated voltage profiles at a specific C-rate and cathode mass loadings (areal capacities), average cell voltages, and total weight or volume of all cell components assuming a combination of 40 cathode/electrolyte/anode layers (see Figure S26 for details). Of note, the cell volume is calculated in the fully discharged state in which Li-garnet SSBs are to be assembled in practice. All parameters contributing to the mass and volume of the cell, such as the thickness of Cu and Al foils and the thickness of pouch Al foil are summarized in Table S3. Thickness of the Li metal anode was fixed, corresponding to 20% of the cathode areal capacity. For instance, Li anode thickness was 1, 3, and 5 μm for cathodic areal capacities of 1, 3, and 5 mAh $cm^{-2}$, accordingly. It should also be pointed out that efficient operation of Li-garnet SSBs with high areal capacities of > 1mAh $cm^{-2}$ can be practically achieved only at stack pressures that enable to mitigate the formation of voids at the LLZO/Li interface.[19–22] As a result, the cell design requires integrating additional inactive components, which severely limits its energy density. Considering the lack of data on the optimal pressure at given current densities and the practical implementation of this requirement, we excluded this parameter from the energy and power density calculations.

Figures 2. (a, b) Simulated voltage profiles of Li/LLZO/LCO all-solid-state battery at different C rates (0.001C, 0.2C, 0.5C, 1C, 2C, and 5C) and temperatures (30°C and 70°C), using cathode constant areal capacity of 4 mAh $cm^{-2}$ and LLZO thickness of 30 μm. (c, d) Gravimetric and volumetric Ragone plots of Li/LLZO/LCO solid-state battery simulated using cathode areal capacities of 0.5, 1, 2, 3, 4, and 5 mAh $cm^{-2}$ at temperatures of 30°C and 70°C and constant LLZO thickness of 30 μm. The simulations were performed using LCO cathode that is composed of 70 vol.% of LCO and 30 vol.% of LLZO.

Next, we analyzed changes of the energy density of the studied solid-state system at gravimetric and volumetric power densities of 200 W $kg^{-1}$ and 600 W $L^{-1}$, corresponding to *ca*. 1h of a full discharge. The data derived from Figures 2c, d and Figures S27-S28 were plotted in the form of 3D maps governing the relationship between areal capacities of LCO cathodes, LLZO thicknesses, and the energy density (Figure 3). Additionally, state-of-the-art values for conventional LIBs are shown in Figure 3 as mesh area, where upper and lowest levels correspond to the energy densities of 18650 Panasonic (231 Wh $kg^{-1}$, 636Wh $L^{-1}$)[41] and Samsung (180 Wh $kg^{-1}$, 497 Wh $L^{-1}$)[42] LIBs at the gravimetric and volumetric power densities of 200 W $kg^{-1}$ and 600 W $L^{-1}$, accordingly. Considering 18650 Samsung battery as a reference system with the minimum necessary electrochemical performance, we identify LLZO thicknesses and areal capacities of Li-garnet SSBs required to match its energy density at 200 W $kg^{-1}$ and 600 W $L^{-1}$. Such values were named break-even thickness and areal capacities, following analogy to the break-even values in economics, representing a set of parameters at which total revenue and total expenses are equal. The break-even areal capacity-thicknesses curves for 30°C and 70°C are indicated in white. As follows from Figure 3a, at 30°C, gravimetric break-even LLZO thickness ranges from 5.5 to 59.5 μm for 1 mAh $cm^{-2}$ and 5 mA $cm^{-2}$, accordingly. However, in the case of 70°C, higher LLZO thicknesses of 5.8 to 86.9 μm (1 mAh

$cm^{-2}$ – 5 mA $cm^{-2}$) can be used in order to reach the same energy density of 180 Wh $kg^{-1}$ at 200 W $kg^{-1}$. The volumetric break-even LLZO thicknesses were very similar at both temperatures: 15.8 – 66.2 μm and 15.7 – 67.5 μm for 0.5 – 1.5 mA $cm^{-2}$ at 30 and 70°C, accordingly.

Notably, considering the employing of a 50 μm LLZO solid-electrolyte membrane, the gravimetric break-even cathode areal capacity equals 3.55, and 3.15 mAh $cm^{-2}$ for the cells at 30°C and 70°C. Volumetric areal capacity of 1.2 mAh $cm^{-2}$ was found to be the break-even value for both temperatures of 30°C and 70°C. Importantly, our calculations show that an increase of the Li anode excess has a moderate impact on the gravimetric energy density of Li-garnet SSBs (Figure S29a, b). For instance, when Li anode thickness was enlarged by a factor of 10, the gravimetric break-even LLZO thickness at a cathode areal capacity of 1.5 mAh $cm^{-2}$ shifted only from 16.8 to 14.9 μm and from 16.8 to 15.4 μm at 30°C and 70°C, accordingly. Correspondingly, at a fixed cathode areal capacity of 1.5 mAh $cm^{-2}$ and LLZO thickness of 15 μm, the gravimetric energy density decreases from 184.4 Wh $kg^{-1}$ and 185.8 Wh $kg^{-1}$ to only 180.2 Wh $kg^{-1}$ and 181.2 Wh $kg^{-1}$ (at 30°C and 70°C). With respect to the volumetric energy density, the picture is the opposite. Ten times higher Li anode amount changes significantly volumetric break-even thicknesses at a cathode areal capacity of 1.5 mAh $cm^{-2}$, from 66.2 μm to 53.2 μm and 67.5 μm to 54.3 μm (at 30°C and 70°C, see Figure S29c, d). As a result, a substantial reduction of the volumetric energy density was found in the case of employing a 10-times thicker Li anode (at a fixed cathode areal capacity of 1.5 mAh $cm^{-2}$ and LLZO thickness of 15 μm): from 939Wh $L^{-1}$ to 774 Wh $L^{-1}$ for 30°C and from 942 Wh $L^{-1}$ to 777 Wh $L^{-1}$ for 70°C.

Subsequently, we analyzed break-even dependences of cathode areal capacity and LLZO thickness for Li/LLZO/LCO solid-state battery on the vol. % of LLZO in LCO solid-state cathode, which are summarized in Figure 4. Figure 4a evidences that upon an increase of LLZO content in a composite cathode, higher areal capacity and lower LLZO solid electrolyte thickness should be used to attain the same energy densities of 180 Wh $kg^{-1}$ and 497 Wh $L^{-1}$ at gravimetric and volumetric power densities of 200 W $kg^{-1}$ and 600 W $L^{-1}$. Interestingly, assuming that the Li-garnet SSBs can be fabricated with 50 μm thick LLZO membrane, 50 vol.% of LLZO fraction in LCO cathode results in gravimetric energy densities not matching the energy density of a conventional Li-ion battery even at very high LCO areal capacity of 4 mAh $cm^{-2}$, requiring LLZO thickness of < 40 μm. In the case of 60 vol.%, the maximal allowed LLZO thickness at LCO areal capacity of 4 mAh $cm^{-2}$ equals 2 μm at 30°C, which can be slightly increased to 7 μm at a higher temperature of 70°C.

With regard to the volumetric performance, already at high LLZO loading of 60 vol. %, relatively thick LLZO membranes of 50 – 90 μm at LCO areal capacities of 1.6 – 2.8 mAh $cm^{-2}$ can be employed to reach volumetric energy density of 497 Wh $L^{-1}$ at 600 Wh $L^{-1}$ (30°C). Based on obtained results, below, we summarize recommended areal capacities of LLZO-LCO cathode at LLZO thickness of 10, 20, 30, and 50 μm and LLZO volumetric content of 30, 40, 50, 60% and temperatures of 30°C or 70°C (Table 1).

Table 1
Recommended areal capacities of LLZO-LCO cathode at given LLZO thickness and vol. % of LLZO in LCO solid-state cathode. Sign "-" means that at given temperature, LLZO thickness and LLZO content in the cathode, the Li-garnet SSB possess lower energy density values than the state-of-the-art value of 180 Wh $kg^{-1}$ at a power density of 200 W $kg^{-1}$.

| T, °C | Vol.% of LLZO in LCO cathode | Thickness of LLZO, µm | Gravimetric break-even areal capacity, mAh $cm^{-2}$ | Volumetric break-even areal capacity, mAh $cm^{-2}$ |
|---|---|---|---|---|
| 30°C | 30% | 20 µm | 1.70 | 0.61 |
| | | 40 µm | 2.84 | 1.03 |
| 70°C | 30% | 20 µm | 1.66 | 0.61 |
| | | 40 µm | 2.64 | 1.03 |
| 30°C | 40% | 20 µm | 2.04 | 0.67 |
| | | 40 µm | 3.67 | 1.1 |
| 70°C | 40% | 20 µm | 1.98 | 0.67 |
| | | 40 µm | 3.18 | 1.1 |
| 30°C | 50% | 20 µm | 2.9 | 0.76 |
| | | 40 µm | - | 1.22 |
| 70°C | 50% | 20 µm | 2.72 | 0.76 |
| | | 40 µm | 4.39 | 1.21 |
| 30°C | 60% | 20 µm | - | 0.91 |
| | | 40 µm | - | 1.43 |
| 70°C | 60% | 20 µm | - | 0.91 |
| | | 40 µm | - | 1.42 |

# Practical challenges towards the fabrication of Li-garnet all-solid-state batteries

Apart from the importance of the above-discussed findings, which highlight the viability of solely garnet SSBs in respect of achievable energy and power densities, adopting the LLZO into the battery cell structure is challenging and requires new approaches in the fabrication of solid-state cathodes and cell design. The latter are primarily related to (i) the intrinsic volume changes of Li anode upon Li plating and stripping and (ii) the chemical reaction of cathode materials with LLZO, yielding non-Li ion conductance phases. These two factors were fully excluded from the simulations.

The volume change of Li is becoming a major challenge when it comes to the deposition of high areal capacities of 1-5 mAh $cm^{-2}$ that correspond to 5-25 μm of Li. This means that, on the one hand, cell design should account for the dynamic expansion of Li anode upon charge. On the other hand, upon discharge, *i.e.*, upon stripping of Li, stack pressure should be applied to the LLZO/Li interface to prevent the formation of cavities, which may arise from the insufficient rate of $Li^+$ diffusion and applied pressure to replenish the Li being dissolved into LLZO.[21] Contrarily, voids can accumulate at the LLZO/Li interface leading to increased local current density and the formation of Li dendrites upon cycling. A rough estimate for the required stack pressure range, provided by Kasemchainan *et al.*,[51] is ca. 10 MPa, allowing to achieve stable cycling at current densities exceeding 1 mA $cm^{-2}$. The external stack pressure is, however, a double-edged sword. Although it seems necessary to inhibit void formation during lithium stripping, some theoretical,[20,52] and experimental reports[53] indicated that stack pressure could lead to quicker cell failure due to increased mechanical stress. Therefore, research is ongoing on finding optimum pressure for Li stripping and the development of cell design enabling to accommodate the dynamical changes in lithium thickness. It should be noted, however, that one possible solution to avoid the Li volume change issue is to use a scaffold-type LLZO, since no external pressure is needed in this case. Thus, Li metal can be plated over the entire surface of the scaffold structure and stored in the pores. As a result, there is no dynamic change in the volume of the cell upon plaiting. Upon stripping, the voids are not forming due to the high surface area of the LLZO/Li interface. Another essential advantage of LLZO scaffolds is the possibility to increase applied current density upon Li plating/stripping up to 10 mA $cm^{-2}$ without the formation of Li dendrites. For instance, as indicated by Wachsmann *et al.*,[54] the current density of 10 mA $cm^{-2}$ for porous LLZO configuration corresponds to the current density of 0.25 mA $cm^{-2}$ for planar configuration, considering that the porous solid-state electrolyte might have up to ~ 40x higher surface area compared to the planar one.

As to the compatibility of LLZO with current cathode chemistries, this issue is mainly caused by the high-temperature co-sintering between LLZO and cathode active materials. For instance, upon heat-treatment of LLZO and $LiCoO_2$ (LCO) cathode above 700°C, insulating decomposition reaction products were reported.[48] High-voltage spinel cathodes ($Li_2NiMn_3O_8$, $Li_2FeMn_3O_8$, and $LiCoMnO_4$) start to react with LLZO even at temperatures as low as 500°C.[55] $LiFePO_4$ (LFP) cathodes are difficult, if not impossible, to co-sinter with LLZO, as LFP phase decomposition already occurs above 400°C.[24] To overcome this compatibility issue, a new design was recently proposed based on wet-chemical infiltration of the cathode active material precursors into porous LLZO solid-state electrolyte, serving as an as-sintered scaffold with their subsequent annealing at lower temperatures.[24] Alternatively, as-synthesized cathode material can be infiltrated into LLZO scaffold, as was demonstrated for $LiNi_{0.6}Mn_{0.2}Co_{0.2}O_2$ (NMC622) particles by Doeff *et al.*[56] Although both methods are interesting, they result in relatively low amounts of active materials, leading to low cathode areal capacities.

# Summary And Outlook

In this work, we analyzed three key contributions to the energy and power densities of Li-garnet solid-state batteries: (i) the LLZO thickness and cathode areal capacity, (ii) Li anode excess, and (iii) the content of LLZO in composite LCO cathodes. We identified the values of each variable that allow the cell to attain the energy density of conventional Li-ion batteries (180 Wh $kg^{-1}$ and 497 Wh $L^{-1}$) at the power density of 200 W $kg^{-1}$ and 600 W $L^{-1}$, corresponding to *ca*. 1 hour of a full discharge. In short, our findings indicate the viability of solely garnet SSB configuration. The detailed conclusions and recommendations are as follows.

First, we reiterate that researchers should focus on Li-garnet SSBs with a small LLZO solid electrolyte thickness of 20 – 50 μm rather than continue reporting on mm-thick LLZO pellets. Only when employing such thin LLZO membranes the state-of-the-art gravimetric and volumetric energy densities of conventional Li-ion batteries at 1h of battery discharge can be attained. Also, working with such thin LLZO thicknesses will aid in identifying at early stages technical challenges in their mass-scale manufacturing. We further note that at LLZO SSE thickness of > 50 μm the employment of cathodes with high areal capacities of > 3 mAh $cm^{-2}$ is imperative for reaching high gravimetric energy densities of 180 Wh $kg^{-1}$ at a power density of 200 Wh $kg^{-1}$. Thus far, the laboratory LLZO-based cells utilized electrodes with very low areal capacities (on average 0.5 – 1 mAh $cm^{-2}$).

Our analysis also concerns the thickness of the Li-metal anode and the content of LLZO in the composite cathodes. Briefly, our calculations show that minimization of the Li excess in Li-garnet SSBs is not very critical for its gravimetric energy density. The employment of thick commercial Li/Cu foils with the Li thickness of *ca*. 50 μm still appears to be a practically viable approach. The content of LLZO in LCO solid-state cathodes should be minimized at least to the level of 30 – 50 vol.% as higher LLZO content requires the deployment of very thin, 2-7 μm LLZO membranes, which is not feasible to achieve experimentally. Additionally, we present recommended minimal areal capacities of LLZO-LCO cathode at given LLZO thickness and vol. % of LLZO in LCO solid-state cathode.

Apart from the cathode loadings, LLZO content in the solid-state cathode, the thicknesses of LLZO SSE, and the metallic Li anode that needs to be adjusted, we highlight that also other aspects of the Li-garnet SSB fabrication should be considered. They are the intrinsic volume changes of Li anode upon its plating and stripping and challenges related to the fabrication of LLZO composed solid-state cathodes. Although it seems that the volume changes of the Li at the anode side can be mitigated either by the employment of pressure or the use of scaffold-type LLZO membranes, it is not yet certain whether it is possible to fabricate solid-state cathodes based on LLZO and Li transition metal oxides, considering their incompatibility upon co-sintering or difficulty in the infiltration of cathode particles in LLZO porous scaffold.

## Declarations

## ACKNOWLEDGMENTS

This research is part of the activities of the joint Empa-Fraunhofer ICS project "IE4B", which is financially supported under the ICON funding scheme.

# Author Contributions

The manuscript was written through contributions of all authors. K.V.K., D.T.K and M.V.K. designed the computational work. D.T.K performed all electrochemical simulations reported in the paper. K.V.K. and M.V.K. wrote the paper. All authors have given approval to the final version of the manuscript.

# Competing Interests:

The authors declare no competing interests.

## References

1. Thangadurai, V., Narayanan, S. & Pinzaru, D. Garnet-type solid-state fast Li ion conductors for Li batteries: critical review. *Chem. Soc. Rev.* **43**, 4714-4727 (2014).
2. Murugan, R., Thangadurai, V. & Weppner, W. Fast lithium ion conduction in garnet-type $Li_7La_3Zr_2O_{12}$. *Angew. Chem., Int. Ed. Engl.* **46**, 7778-7781 (2007).
3. Ohta, S., Kobayashi, T. & Asaoka, T. High lithium ionic conductivity in the garnet-type oxide $Li_{7-X}La_3(Zr_{2-X}, Nb_X)O_{12}$ (X=0–2). *J. Power Sources* **196**, 3342-3345 (2011).
4. Allen, J. L., Wolfenstine, J., Rangasamy, E. & Sakamoto, J. Effect of substitution (Ta, Al, Ga) on the conductivity of $Li_7La_3Zr_2O_{12}$. *J. Power Sources* **206**, 315-319 (2012).
5. Ohta, S., Kihira, Y. & Asaoka, T. Spontaneous formation of a core–shell structure by a lithium ion conductive garnet-type oxide electrolyte for co-sintering with the cathode. *J. Mater. Chem. A* (2021).
6. Buschmann, H., Berendts, S., Mogwitz, B. & Janek, J. Lithium metal electrode kinetics and ionic conductivity of the solid lithium ion conductors "$Li_7La_3Zr_2O_{12}$" and $Li_{7-x}La_3Zr_{2-x}Ta_xO_{12}$ with garnet-type structure. *J. Power Sources* **206**, 236-244 (2012).
7. Buschmann, H.*et al.* Structure and dynamics of the fast lithium ion conductor "$Li_7La_3Zr_2O_{12}$". *Phys. Chem. Chem. Phys.* **13**, 19378-19392 (2011).
8. Taylor, N. J.*et al.* Demonstration of high current densities and extended cycling in the garnet $Li_7La_3Zr_2O_{12}$ solid electrolyte. *J. Power Sources* **396**, 314-318 (2018).
9. Samson, A. J., Hofstetter, K., Bag, S. & Thangadurai, V. A bird's-eye view of Li-stuffed garnet-type $Li_7La_3Zr_2O_{12}$ ceramic electrolytes for advanced all-solid-state Li batteries. *Energy Environ. Sci.* **12**, 2957-2975 (2019).
10. Afyon, S.*et al.* Building better all-solid-state batteries with Li-garnet solid electrolytes and metalloid anodes. *J. Mater. Chem. A* **7**, 21299-21308 (2019).

11. Randau, S.*et al.* Benchmarking the performance of all-solid-state lithium batteries. *Nat. Energy* **5**, 259-270 (2020).
12. Rangasamy, E., Wolfenstine, J. & Sakamoto, J. The role of Al and Li concentration on the formation of cubic garnet solid electrolyte of nominal composition $Li_7La_3Zr_2O_{12}$. *Solid State Ion.* **206**, 28-32 (2012).
13. Thangadurai, V., Pinzaru, D., Narayanan, S. & Baral, A. K. Fast solid-state Li ion conducting garnet-type structure metal oxides for energy storage. *J. Phys. Chem. Lett.* **6**, 292-299 (2015).
14. Zhao, N.*et al.* Solid garnet batteries. *Joule* **3**, 1190-1199 (2019).
15. Shen, X.*et al.* Critical challenges and progress of solid garnet electrolytes for all-solid-state batteries. *Mater. Today Chem.* **18**, 100368 (2020).
16. Duan, H.*et al.* Li/Garnet interface optimization: An overview. *ACS Appl. Mater. Interfaces* **12**, 52271-52284 (2020).
17. Kim, A., Woo, S., Kang, M., Park, H. & Kang, B. Research progresses of garnet-type solid electrolytes for developing all-solid-state Li batteries. *Front. Chem.* **8** (2020).
18. Xu, L.*et al.* Garnet solid electrolyte for advanced all-solid-state Li batteries. *Adv. Energy Mater.* **11**, 2000648 (2021).
19. Wang, M. J., Choudhury, R. & Sakamoto, J. Characterizing the Li-solid-electrolyte interface dynamics as a function of stack pressure and current density. *Joule* **3**, 2165-2178 (2019).
20. Zhang, X., Wang, Q. J., Harrison, K. L., Roberts, S. A. & Harris, S. J. Pressure-driven interface evolution in solid-state lithium metal batteries. *Cell Rep. Phys. Sci.* **1**, 100012 (2020).
21. Krauskopf, T., Hartmann, H., Zeier, W. G. & Janek, J. Toward a fundamental understanding of the lithium metal anode in solid-state batteries—an electrochemo-mechanical study on the garnet-type solid electrolyte $Li_{6.25}Al_{0.25}La_3Zr_2O_{12}$. *ACS Appl. Mater. Interfaces* **11**, 14463-14477 (2019).
22. Krauskopf, T., Richter, F. H., Zeier, W. G. & Janek, J. Physicochemical concepts of the lithium metal anode in solid-state batteries. *Chem. Rev.* **120**, 7745-7794 (2020).
23. Kim, K. J., Balaish, M., Wadaguchi, M., Kong, L. & Rupp, J. L. M. Solid-state Li–metal batteries: challenges and horizons of oxide and sulfide solid electrolytes and their interfaces. *Adv. Energy Mater.* **11**, 2002689 (2021).
24. Kim, K. J. & Rupp, J. L. M. All ceramic cathode composite design and manufacturing towards low interfacial resistance for garnet-based solid-state lithium batteries. *Energy Environ. Sci.* **13**, 4930-4945 (2020).
25. Han, F.*et al.* Interphase engineering enabled all-ceramic lithium battery. *Joule* **2**, 497-508 (2018).
26. Liu, T.*et al.* Achieving high capacity in bulk-type solid-state lithium ion battery based on $Li_{6.75}La_3Zr_{1.75}Ta_{0.25}O_{12}$ electrolyte: Interfacial resistance. *J. Power Sources* **324**, 349-357 (2016).
27. Liu, T.*et al.* Enhanced electrochemical performance of bulk type oxide ceramic lithium batteries enabled by interface modification. *J. Mater. Chem. A* **6**, 4649-4657 (2018).

28. Ren, Y., Liu, T., Shen, Y., Lin, Y. & Nan, C.-W. Garnet-type oxide electrolyte with novel porous-dense bilayer configuration for rechargeable all-solid-state lithium batteries. *Ionics* **23**, 2521-2527 (2017).
29. Kato, T.*et al.* Preparation of thick-film electrode-solid electrolyte composites on $Li_7La_3Zr_2O_{12}$ and their electrochemical properties. *J. Power Sources* **303**, 65-72 (2016).
30. Ohta, S.*et al.* All-solid-state lithium ion battery using garnet-type oxide and $Li_3BO_3$ solid electrolytes fabricated by screen-printing. *J. Power Sources* **238**, 53-56 (2013).
31. Liu, T.*et al.* Non-successive degradation in bulk-type all-solid-state lithium battery with rigid interfacial contact. *Electrochem. commun.* **79**, 1-4 (2017).
32. Inada, R.*et al.* Development of lithium-stuffed garnet-type oxide solid electrolytes with high ionic conductivity for application to all-solid-state batteries. *Front. Energy Res.* **4** (2016).
33. Shao, Y.*et al.* Drawing a soft interface: an effective interfacial modification strategy for garnet-type solid-state Li batteries. *ACS Energy Lett.* **3**, 1212-1218 (2018).
34. Pervez, S. A.*et al.* Overcoming the interfacial limitations imposed by the solid–solid interface in solid-state batteries using ionic liquid-based interlayers. *Small* **16**, 2000279 (2020).
35. Takemoto, K., Wakasugi, J., Kubota, M., Abe, H. & Kanamura, K. Lithium-sulfur batteries employing hybrid-electrolyte structure with $Li_7La_3Zr_2O_{12}$ at middle operating temperature: effect of Li salts concentration on electrochemical performance. *Electrochemistry* **89**, 197-203 (2021).
36. Huo, H.*et al.* In-situ formed $Li_2CO_3$-free garnet/Li interface by rapid acid treatment for dendrite-free solid-state batteries. *Nano Energy* **61**, 119-125 (2019).
37. Dubey, R.*et al.* Building a better Li-garnet solid electrolyte/metallic Li interface with antimony. *Adv. Energy Mater.*, 2102086 (2021).
38. Wang, M. J., Carmona, E., Gupta, A., Albertus, P. & Sakamoto, J. Enabling “lithium-free” manufacturing of pure lithium metal solid-state batteries through in situ plating. *Nat. Commun.* **11**, 5201 (2020).
39. Sharafi, A., Haslam, C. G., Kerns, R. D., Wolfenstine, J. & Sakamoto, J. Controlling and correlating the effect of grain size with the mechanical and electrochemical properties of $Li_7La_3Zr_2O_{12}$ solid-state electrolyte. *J. Mater. Chem. A* **5**, 21491-21504 (2017).
40. Kravchyk, K. V., Okur, F. & Kovalenko, M. V. Break-even analysis of all-solid-state batteries with Li-garnet solid electrolytes. *ACS Energy Lett.*, 2202-2207 (2021).
41. https://www.batteryspace.com/prod-specs/NCR18650B.pdf. Panasonic 18650 Datasheet
42. Zhang, Y. C.*et al.* Non-isothermal Ragone plots of Li-ion cells from datasheet and galvanostatic discharge tests. *Applied Energy* **247**, 703-715 (2019).
43. Ménétrier, M., Saadoune, I., Levasseur, S. & Delmas, C. The insulator-metal transition upon lithium deintercalation from $LiCoO_2$: electronic properties and $^7Li$ NMR study. *J. Mater. Chem.* **9**, 1135-1140 (1999).
44. Tukamoto, H. & West, A. R. Electronic conductivity of $LiCoO_2$ and its enhancement by magnesium doping. *J. Electrochem. Soc.* **144**, 3164-3168 (1997).

45. Molenda, J., Wilk, P. & Marzec, J. Structural, electrical and electrochemical properties of $LiNiO_2$. *Solid State Ion.* **146**, 73-79 (2002).
46. Amin, R., Ravnsbæk, D. B. & Chiang, Y.-M. Characterization of Electronic and Ionic Transport in $Li_{1-x}Ni_{0.8}Co_{0.15}Al_{0.05}O_2$(NCA). *J. Electrochem. Soc.* **162**, A1163-A1169 (2015).
47. COMSOL Multiphysics® v. 6. www.comsol.com. COMSOL AB, S., Sweden.
48. Ren, Y., Liu, T., Shen, Y., Lin, Y. & Nan, C.-W. Chemical compatibility between garnet-like solid state electrolyte $Li_{6.75}La_3Zr_{1.75}Ta_{0.25}O_{12}$ and major commercial lithium battery cathode materials. *J. Mater.* **2**, 256-264 (2016).
49. Krauskopf, T.*et al.* The fast charge transfer kinetics of the lithium metal anode on the garnet-type solid electrolyte $Li_{6.25}Al_{0.25}La_3Zr_2O_{12}$. *Adv. Energy Mater.* **10**, 2000945 (2020).
50. Sastre, J., Chen, X., Aribia, A., Tiwari, A. N. & Romanyuk, Y. E. Fast charge transfer across the $Li_7La_3Zr_2O_{12}$ solid electrolyte/$LiCoO_2$ cathode interface enabled by an interphase-engineered all-thin-film architecture. *ACS Appl. Mater. Interfaces* **12**, 36196-36207 (2020).
51. Kasemchainan, J.*et al.* Critical stripping current leads to dendrite formation on plating in lithium anode solid electrolyte cells. *Nat. Mater.* **18**, 1105-1111 (2019).
52. Sakamoto, J. More pressure needed. *Nat. Energy* **4**, 827-828 (2019).
53. Doux, J.-M.*et al.* Stack pressure considerations for room-temperature all-solid-state lithium metal batteries. *Adv. Energy Mater.* **10**, 1903253 (2020).
54. Hitz, G. T.*et al.* High-rate lithium cycling in a scalable trilayer Li-garnet-electrolyte architecture. *Mater. Today* **22**, 50-57 (2019).
55. Miara, L.*et al.* About the compatibility between high voltage spinel cathode materials and solid oxide electrolytes as a function of temperature. *ACS Appl. Mater. Interfaces* **8**, 26842-26850 (2016).
56. Shen, H.*et al.* Oriented porous LLZO 3D structures obtained by freeze casting for battery applications. *J. Mater. Chem. A* **7**, 20861-20870 (2019).

# Figures

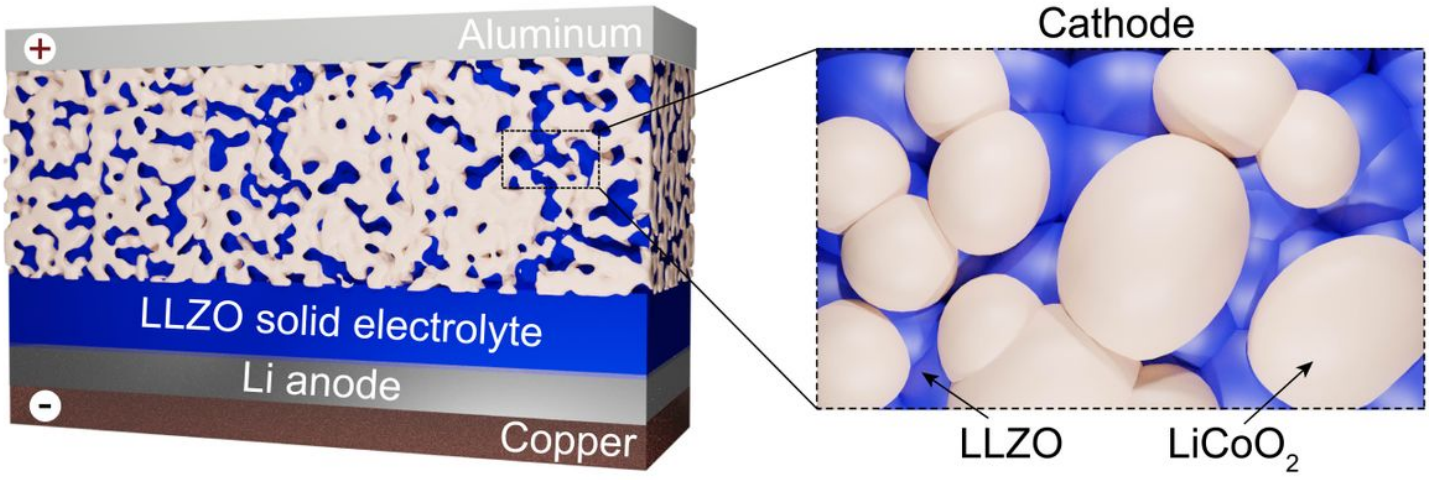

## Figure 1

Schematics of Li-garnet solid-state battery and solid-state cathode considered in this work for assessing the power and energy densities of Li-garnet SSBs.

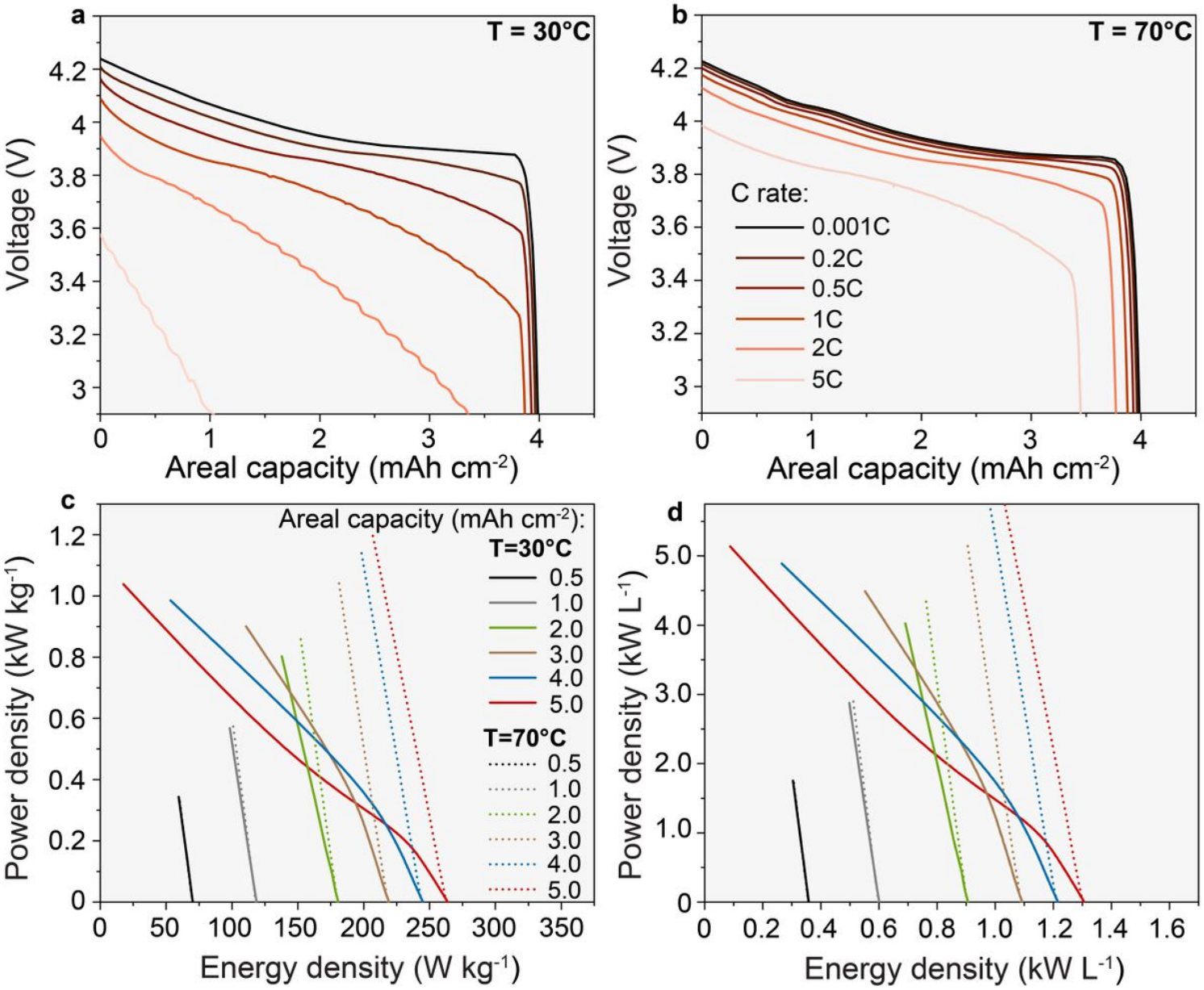


## Figure 2

(a, b) Simulated voltage profiles of Li/LLZO/LCO all-solid-state battery at different C rates (0.001C, 0.2C, 0.5C, 1C, 2C, and 5C) and temperatures (30 °C and 70 °C), using cathode constant areal capacity of 4 mAh cm-2 and LLZO thickness of 30 µm. (c, d) Gravimetric and volumetric Ragone plots of Li/LLZO/LCO solid-state battery simulated using cathode areal capacities of 0.5, 1, 2, 3, 4, and 5 mAh cm-2 at temperatures of 30 °C and 70 °C and constant LLZO thickness of 30 µm. The simulations were performed using LCO cathode that is composed of 70 vol.% of LCO and 30 vol.% of LLZO.

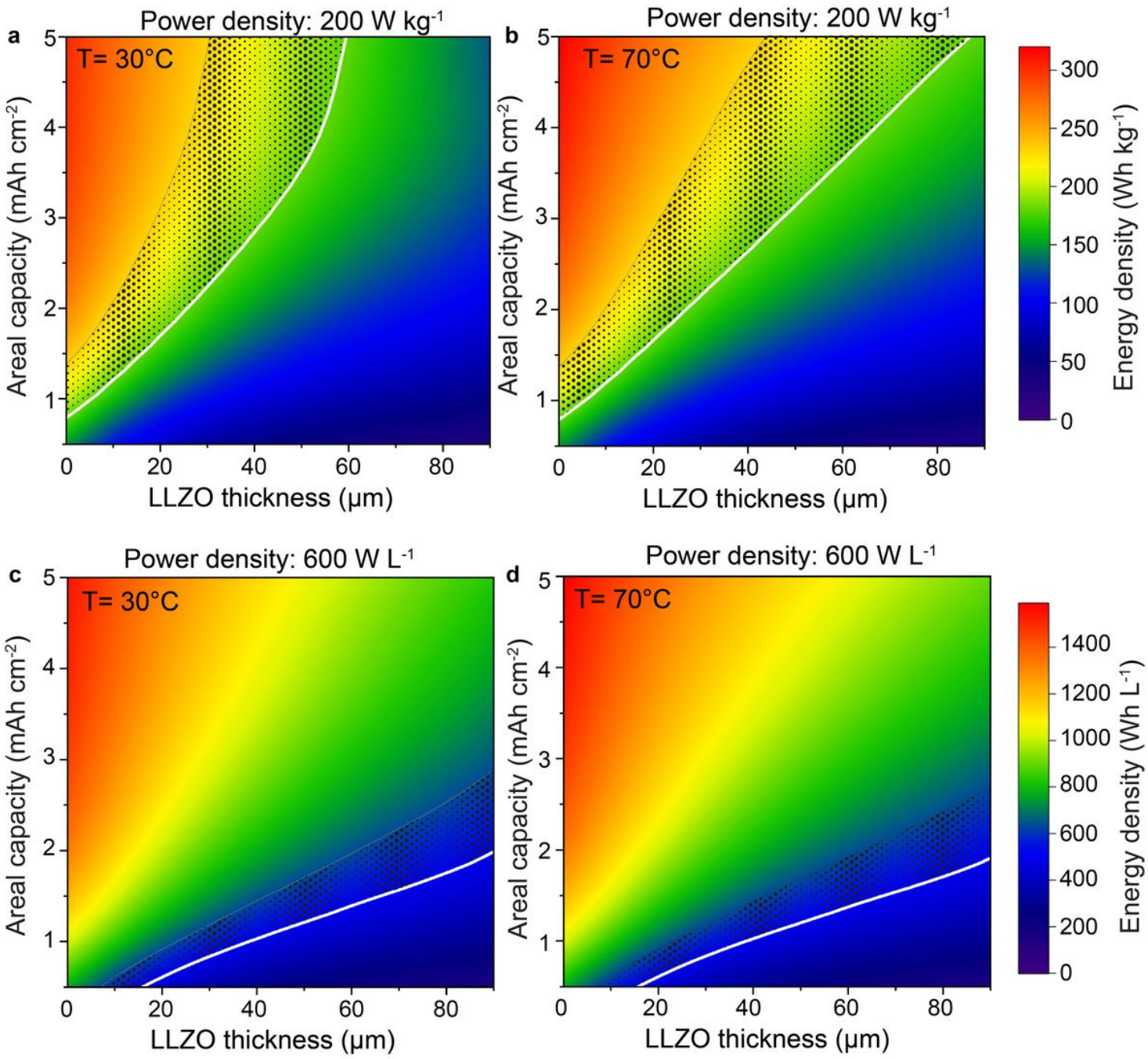


## Figure 3

Simulated gravimetric (a, b) and volumetric (c, d) energy densities of Li/LLZO/LCO all-solid-state battery vs. cathode areal capacity and LLZO thickness plotted at power densities of 200 W kg-1 and 600 W L-1 and temperatures of 30 °C and 70 °C. The composition of LCO cathode is constant (70 vol.% of LCO and 30 vol.% of LLZO). The areal capacity (thickness) of the Li metal anode corresponds to 20% of the cathode areal capacity.

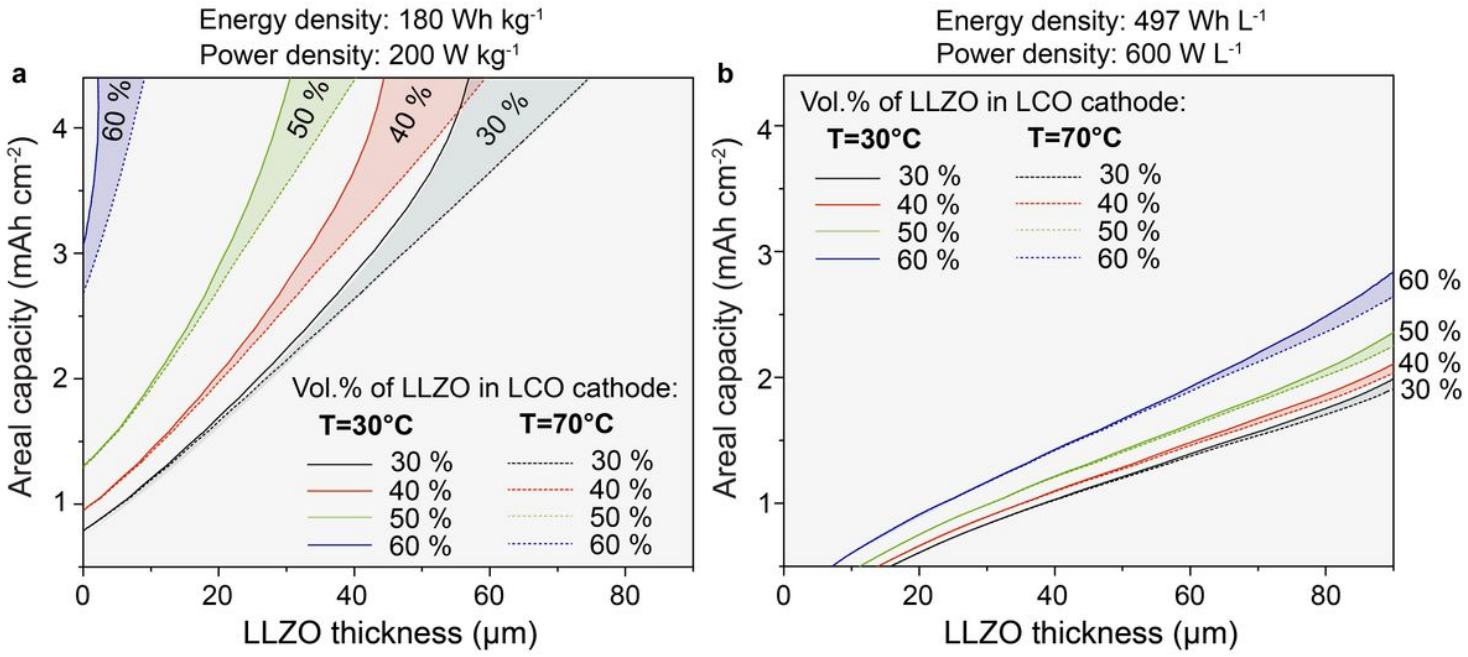


**Figure 4**

Gravimetric and volumetric break-even dependence of cathode areal capacity and LLZO thickness for Li/LLZO/LCO solid-state battery comprising LCO cathode with different volumetric content of LLZO. These dependencies were derived from simulated voltage profiles shown on Figures S2-S7, S8-S13, S14-S19, and S20-S25 and corresponding Ragone plots shown on Figures S27-S28, S30-S31, S32-S33, and S34-S35 (for 30, 40, 50, and 60 vol. % of LLZO in LCO). Complete sets of data of simulated energy densities are shown on Figure 3 (70 vol.% of LCO and 30 vol.% of LLZO), Figure S36 (60 vol.% of LCO and 40 vol.% of LLZO), Figure S37 (50 vol.% of LCO and 50 vol.% of LLZO), and Figure S38 (40 vol.% of LCO and 60 vol.% of LLZO).

# Supplementary Files

This is a list of supplementary files associated with this preprint. Click to download.

- SI.docx